Unveiling the Pitfalls of Comparing ORR Kinetic Data for Pd-Based Electrocatalysts without the Experimental Conditions of the Current–Potential Curves

Yaovi Holade, Qing Wang, Hazar Guesmi, Sophie Tingry, David Cornu, Shelley Minteer

Unveiling the Pitfalls of Comparing ORR Kinetic Data for Pd-based Electrocatalysts Without the Experimental Conditions of the Current-Potential Curves

Yaovi Holade,[1,] Qing Wang,[2] Hazar Guesmi,[2] Sophie Tingry,[1] David Cornu,[1] and Shelley D. Minteer[3,*]*

[1]Institut Européen des Membranes, IEM, UMR 5635, Univ Montpellier, ENSCM, CNRS, 34090 Montpellier, France.

[2]ICGM, UMR 5253, Univ Montpellier, CNRS, ENSCM, Montpellier, France

[3]Departments of Chemistry, University of Utah, Salt Lake City, Utah 84112, USA

AUTHOR INFORMATION

Corresponding Authors

*Y.H.: E-mail: yaovi.holade@enscm.fr; *S.D.M.: E-mail: minteer@chem.utah.

The road to solid-polymer-electrolyte fuel cells[1] relies on the sluggish electrocatalytic reduction of oxygen (ORR)[2] that bridges the fields of metal-air batteries and alkaline fuel cells. Among many electrocatalysts being explored each year, only Pd can replace Pt with akin ORR activity in alkaline media [$O_2 + 2H_2O + 4e^- \rightarrow 4HO^-$, E_{eq} ~1.18 V_{RHE} (RHE: reversible hydrogen electrode)],[3-4] thus the option to reduce the economic stress on Pt alone. As any electrocatalytic reaction, ORR's main metrics[2,5-8] are the kinetic current density (j_k, A mg^{-1}_{metal} or A cm^{-2}_{ECSA}, ECSA = electrochemically active surface area), the Tafel slope (b, mV dec^{-1}, potential required to achieve 10-fold increase, its interpretation is more complex[6]), the half-wave potential ($E_{1/2}$, potential for a half value of the limiting current), the onset potential (E_{onset}, potential at which ORR starts) and the exchange current density (j_0). The higher j_k ($E_{1/2}$, E_{onset} and j_0) is, the more active the electrocatalyst is. Although some testing protocols or "best practices" are reported,[5,7-9] a deep analysis of the literature points out an impossibility for a fair comparison of ORR kinetic parameters due to a lack of full disclosure of experimental conditions. The latter is, however, essential to "cross the valley of death"[10] in scientific research from fundamental to applied fields. In 0.1 $HClO_4$, Shinozaki *et al.*[9] used the method of linear sweep voltammetry (LSV) to reveal that $j_{k,anodic}$ of the anodic sweep (from lower to higher potential) is considerably higher than $j_{k,cathodic}$ of the cathodic sweep (from higher to lower potential): at 0.9 V_{RHE}, $j_{k,anodic}/j_{k,cathodic}$ = 5.3 (bulk Pt) and 2.4 (nano Pt). Our recent data show a huge discrepancy, $j_{k,anodic}/j_{k,cathodic}$ of an order of magnitude for supported PdFe electrocatalysts in 0.1 M KOH.[11] The summarized random sample of publications in alkaline media (period of 2015-2021) in Table S1 clearly shows that the majority of the reports do not state the scan direction and/or do not use the same protocol,[3,12-15] which means a conflicting comparison of the activity where a claimed outstanding performance or superiority over the others could not be.

While a plethora of Pd-based electrocatalysts are synthesized every year for ORR in alkaline media, research questions of fundamental importance are still unanswered: (i) what should be the best way to evaluate their performance and compare them to those already existing? (ii) to what extent the comparison is biased if, to record the current-potential polarization curves of ORR using a rotating disk/ring electrode (RDE/RRDE), the scan direction (anodic vs cathodic), the scan rate (5 to 50 mV s^{-1}) and the scan nature (LSV vs CV) are not clearly made explicit? This Viewpoint aims to answer these questions and draw the attention of researchers to experimental situations that can lead to an erroneous evaluation/comparison of ORR kinetic parameters for Pd-based electrocatalysts in alkaline media. We have performed a set of experiments at the forefront of electrochemical, electrocatalytic and computational sciences to: (i) interrogate current practices by using commercial Pd/C, (ii) and encourage researchers to adopt transparency and reproducible methodologies in fundamental and applied research in energy conversion systems.

Figure 1 clearly shows that if two persons do use the same scan direction during LSV to record ORR data, they will claim different performance, however, it is the same electrocatalyst Pd/C.

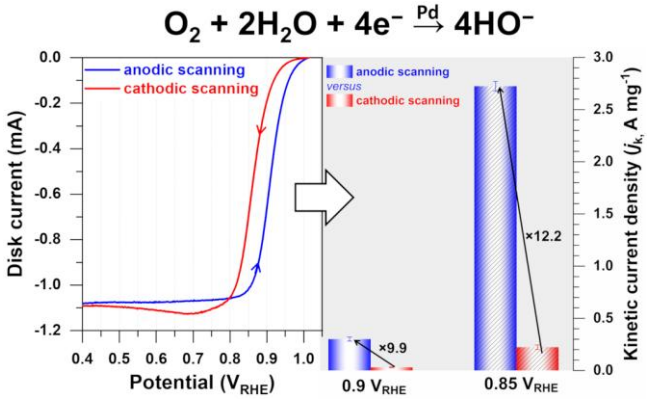

Figure 1. ORR kinetic activity extracted from the anodic scanning [from 0.35 V_{RHE} to OCP (ca. 1.05 V_{RHE})] looks "superior" to that found from the cathodic scanning [from OCP (ca. 1.05 V_{RHE}) to 0.35 V_{RHE}] in 0.1 M KOH at Pd/C [50 μg_{Pd} cm^{-2}, 5 mV s^{-1}, 1600 rpm, room temperature (23 ± 2 °C)]. The leading experimental causes are discussed in this Viewpoint.

As the kinetic activity of ORR is size-/shape-dependent,[16] we firstly used transmission electron microscopy (TEM) to precisely characterize the commercial electrocatalyst of carbon black supported Pd (Pd/C, 20 wt.% Pd loading, 3-4 nm crystallites size, Premetek Co., USA). Figure 2a shows the high-resolution TEM image of an individual Pd particle of 3.2 ± 0.1 nm that is consistent with the supplier's data (Figures S2-S6 for extended data). The interplanar space of 0.23 nm implies the predominance of the Pd(111) crystalline plane. Based on this finding, theoretical and computational investigations on Pd model semi-infinite surface were considered to gain insights into the interaction of the O_2 molecule with the electrocatalyst surface.

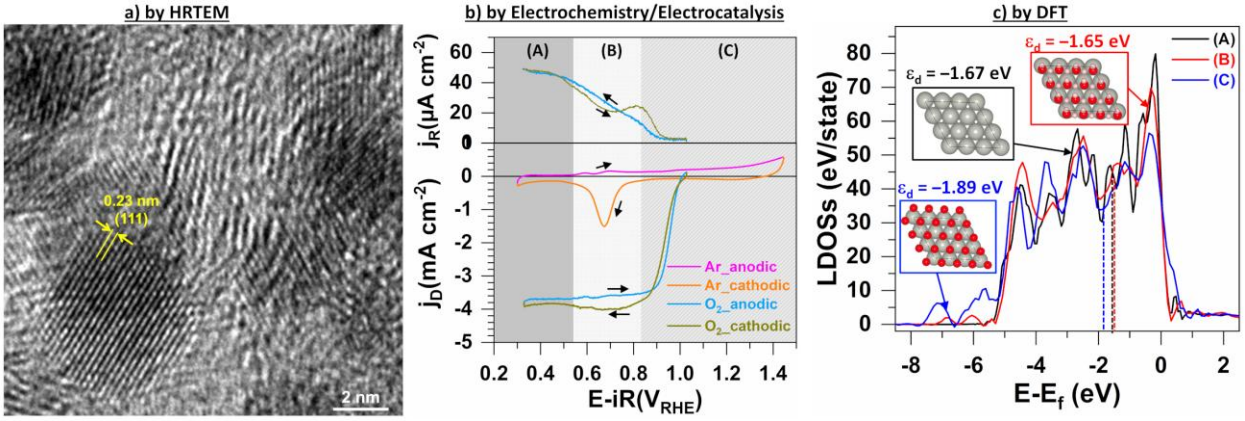

Figure 2. (a) TEM of Pd/C. (b) Steady-state CV recorded at RRDE in the presence and presence of O_2 (1 M KOH, 1600 rpm, 10 mV s^{-1}): anodic direction vs cathodic direction. (c) DFT calculated Local Density of States (LDOSs) of the Pd 4*d* bands in the three modelled systems (inserts), (A) pristine Pd(111), (B) hydroxylated Pd(111) and (C) oxidized Pd(111).

To better understand the electrocatalysis of ORR using RRDE [disk = 0.196 cm^2 glassy carbon disk coated with 50 μg_{Pd} cm^{-2}, ring = 0.072 cm^2 Pt bulk], cyclic voltammetry (CV) experiments were recorded in the absence and presence of O_2. Figure 1b shows that if two different studies did not use the same scan directions, they will report different behaviors and performance for j_k;

however, it is the same electrocatalyst. Figure 2b shows that in the outgassed electrolyte (lower potential limit fixed at 0.3 V_{RHE} to avoid hydride formation for lower values[17-18]), Pd reacts with OH^- to produce $Pd(OH)_x$ (from 0.52 V_{RHE}) that further evolves into PdO (from 0.69 V_{RHE}), and the latter is reduced back to metallic Pd with a peak at 0.67 V_{RHE} (the monolayer charge of 424 μC cm^{-2} for 1.45 V_{RHE} upper potential limit is used to calculate ECSA).[18-19] Under O_2 with an OCP of ca. 1.03 V_{RHE}, the forward (from 0.35 V_{RHE} to OCP) and backward (from OCP to 0.35 V_{RHE}) scans give 3 domains of the current density of the disk (bottom) and ring (top). RRDE has a collection efficiency of 24.5 ± 0.5% (Figure S7) and will enable quantifying the incomplete hydroperoxide anion HO_2^- in alkaline media ($pK_a(H_2O_2/HO_2^-)$ = 11.75) and the overall number of exchanged electrons using Eqs. S1-S11. First, the activation region at high potential (low overpotential, characterized by E_{onset}) where the reaction rate is limited by the electrons transfer from the electrocatalyst surface to O_2. Second, the diffusion-limiting region at low potential [high overpotential, characterized by a limiting current density j_{diff} (Levich's relationship), Table S2] where the rate is limited by the mass transport of O_2 from the bulk electrolyte to active sites. Third, the mixed kinetic-diffusion controlled region (characterized by $E_{1/2}$) where the Koutecky-Levich model [with two implicit criteria, *the existence of an electron transfer process that is the rate-determining step (rds)* and *a first-order reaction with respect to O_2*][20] enables to extract the kinetic data from the potential region corresponding to $0.1 \times j_{diff} < j < 0.8 \times j_{diff}$.[8] E_{onset} should be considered for $j < 0.01 \times j_{diff}$. The more positive E_{onset} (high) is, the more active the electrocatalyst is because the cell voltage is $U = E_{(cathode)} - E_{(anode)}$, so a high $E_{(cathode)}$ is sought for ORR.

We note that these control experiments in the absence and presence of O_2 enable us to clearly distinguish three domains: (A) metal-based surface, (B) hydroxyl-based surface and (C) oxide-based surface. Similar to Pt(111) that is the model electrocatalytic surface for ORR, and based on

the above characterization, we next performed first principle Density Functional Theory (DFT) calculations to reveal how the nature of the Pd electrocatalyst surface (thus the potential range) modifies its interaction with O_2 molecule and strongly impacts the measured kinetic activity. Figure 2c shows the computed local density of states (LDOS) of the 4*d*-bands of Pd atoms in three modelled systems (A) pristine, (B) hydroxylated and (C) oxidized Pd(111) surfaces (see inserts). From these curves, the *d*-band center (ε_d, relative to the Fermi level) may be used as a descriptor of surface reactivity. Here, it can be seen that the *d*-band centers ε_d of oxidized Pd(111) (-1.89 eV) is highly shifted away from the Fermi level compared to ε_d of Pd(111) (-1.67 eV) and ε_d of hydroxylated Pd(111) (-1.65 eV) which indicate stronger bonding of O_2 over the latter two surfaces. According to Nørskov theory,[21] the *d*-band centers position toward the Fermi level may be correlated to the interaction with adsorbates; the closer the position of ε_d toward the Fermi level, the stronger the interactions with adsorbates. This correlation is confirmed by the calculated binding energies of O_2 on the three selected systems (see Table S3), -0.99 eV on pristine Pd(111), -1.01 eV on hydroxylated Pd(111) and -0.12 eV on the oxidized Pd(111). The computed geometric parameters of O_2 suggest that O_2 does not strongly interact with the oxidized Pd(111) because the O-O bond distance is 1.33, 1.27 and 1.23 Å [2.04–2.06, 2.13, 3.66 Å for the distance of O_2 from the surface] for metallic Pd(111), hydroxylated Pd(111) and oxidized Pd(111), respectively. The stronger adsorption energies of O_2 together with the elongated O-O band distances on metallic and hydroxylated Pd(111) suggest that the barriers for O_2 dissociation are much lower on these surfaces than on oxidized one. Moreover, these results confirm the experimentally distinguished three regions of palladium surface engaged in the ORR (metallic vs hydroxylated vs oxidized), which means that the full experimental conditions related to the electrode potential scanning should be always provided for a fair comparison.

Impact of the scan direction (potential sweep): anodic vs cathodic. The preceding results have shown that for a fixed potential range, e.g. 0.3-1 V_{RHE}, the starting point immediately changes the surface state. This consequently affects the nature of the "electrocatalyst-O_2" interaction and thus the electrocatalytic activity, but we currently lack data on the extent of the discrepancy. So, to provide representative results based on the current research practices, we have used two concentrations of the electrolyte, which are 0.1 and 1 M KOH. Data of Table S2 show that for $4e^-$ ORR at 1600 rpm, j_{diff}(mA cm^{-2}) = -5.7 and -3.6 for 0.1 and 1 M, respectively. While 0.1 M is routinely used, 1 M is closer to the realistic OH^- concentration in practical situations.[22] In 1 M KOH, j_{diff} is low because of the reduced solubility and diffusion coefficient of O_2 in bulk electrolyte.[3,23] Figure 3a shows that, regardless of the electrolyte concentration, the LSV curves (1600 rpm, 5 mV s^{-1}) shift to higher potentials in the kinetic region ($E \geq 0.8$ V_{RHE}). This is supported by a drastic change of the kinetic parameters when switching from the cathodic to anodic direction (Figures 3b-e, S8-S9, Table S2). For $E_{1/2}$ (Figure 3b), $\Delta E_{1/2,anodic/cathodic}$ = 42-51 mV. For j_k (Figures 3c-d), $j_{k,anodic}/j_{k,cathodic}$ = 10.0 (0.1 M KOH) and 7.7 (1 M KOH) at 0.90 V_{RHE}, while at 0.85 V_{RHE}, $j_{k,anodic}/j_{k,cathodic}$ = 12.2 (0.1 M KOH) and 2.8 (1 M KOH). There is a slight decrease of the Tafel slope of $\Delta b_{anodic/cathodic}$ = 5-10 mV dec^{-1} (Figure 3d). Figures 3f and S9a show that the scan direction impacts the mechanism of ORR with a high amount of HO_2^- from the incomplete ORR ($O_2 + H_2O + 2e^- \rightarrow HO_2^- + OH^-$) when considering the cathodic scan. This could already be seen in Figure 3a with the current recorded at the Pt ring for its oxidation back into O_2. Even though, herein, the overall transferred number of electrons per O_2 molecule is closed to 4 (Figure S9b), for fuel cells applications,[2] hydrogen peroxide species are not desired because their accumulation throughout the operation will diminish the performance and the lifetime by decreasing the faradaic efficiency and the durability of the solid polymer membranes.

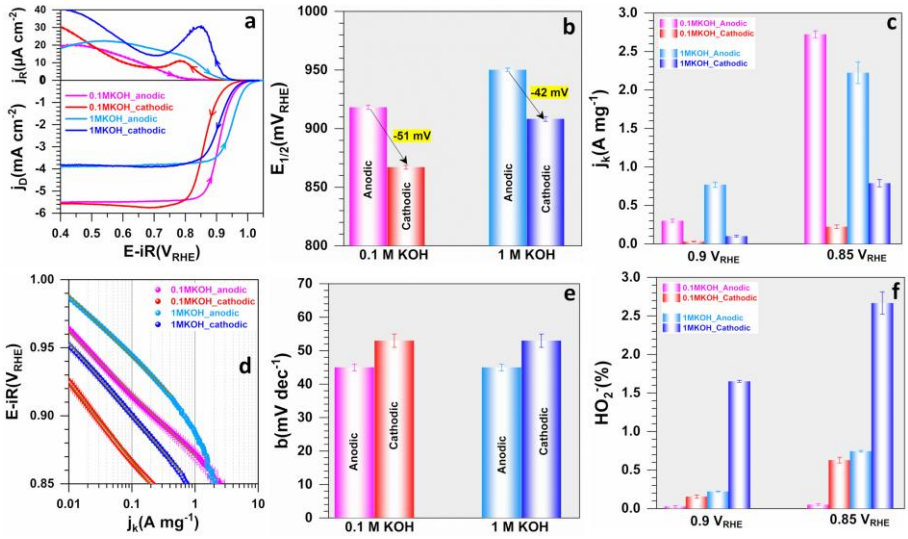

Figure 3. Scan direction effect. (a) LSV (1600 rpm, 5 mV s^{-1}) of ORR at an RRDE: disk (bottom) and ring (top). (b) Half-wave potential. (c) Kinetic current density. (d) Tafel plots. (e) Tafel slope. (f) Incomplete hydroperoxide anion. Error bars represent 1 SD ($n \geq 3$).

Based on the previous electrochemistry and DFT data, the origin of this discrepancy is the surface state of the electrocatalyst, depending on where LSV starts. For the cathodic direction, the sweep begins in a region where the electrocatalyst surface is covered by oxidized species and subsequently, the reduction of these species and O_2 proceeds concomitantly. This can be seen in Figures 2a and 3a with a small deviation of the current around 0.7 V_{RHE} leading to a high plateau. For the anodic direction, the scan starts from metallic surface and subsequently builds up as the potential increases from reducing to oxidizing.[9] The result is the change of the electrocatalyst-O_2 interface caused by several sources such as the nature of actives sites [Pd, $Pd(OH)_x$, PdO]. The latter means a change in the types of electronic interaction and charge transfer resistance as well as the available number of actives sites and ECSA. These results demonstrate that when researchers do not specify the direction in which the LSV curves were obtained, the comparison of performance cannot be fair. Or, when reporting ORR data, it is not relevant to compare data

obtained by one direction with another direction (disclosed or not) because we have seen here in alkaline media (elsewhere in acidic media[9]) that we have 2 to 12 times difference in activity. One can, unfortunately, notice that, for manuscripts on ORR, the tables summarizing the comparison with previous data by other researchers never mention the used scan direction. That said, when not disclosed, the probability that it would be the same scan direction is 50%, which is not trivial. For everybody, the baseline of comparison must be the same, which is unfortunately not the case as summarized in Table S1 for a random sample of publications in alkaline media (2015-2021).

Impact of the scan rate. Having shown that the scan direction during LSV affects dramatically the magnitude of the measured kinetic metrics of ORR because of the dependence on the oxidation state of palladium surface, we next interrogated the possible impact of the scan rate by using 50, 20, 10 and 5 mV s^{-1}. This is very important because, for a fixed potential range, the electrocatalyst will spend more time in each of the above three regions at low scan rates. While 5 mV s^{-1} should be closed to the pseudo steady-state, 50 mV s^{-1} appears to be too fast (10 times). This means that not all the oxidized species of the palladium will be reduced at higher scan rates as confirmed by LSV curves in Figures S10a and S11a (the undesired HO_2^- amount is incredibly high for the cathodic direction), making it difficult in extracting reliable kinetic data for scan rates higher than 20 mV s^{-1}. We note that Shinozaki *et al.*[9] have observed the reverse trend in 0.1 M $HClO_4$ at Pt where the kinetic data systematically decrease upon the increase of the scan rate. Here, while the extracted kinetic data in both electrolytes clearly highlight a big difference between the anodic and cathodic directions (Figures 4, S10 and S11), there is no monotonous evolution of the kinetics. This is possible because of the nature of the electrolyte, the active sites and the catalytic metal. Overall, 10 mV s^{-1} appears to be the best compromise for the tested conditions. At 10 mV s^{-1}, $j_{k,anodic}/j_{k,cathodic}$ = 14.0 (0.1 M KOH) and 5.5 (1 M KOH) at 0.90 V_{RHE}

while $\Delta E_{1/2,\text{anodic/cathodic}}$ = 43 mV and $\Delta b_{\text{anodic/cathodic}}$ = 5-5 mV dec^{-1}. All this confirms that the literature comparison should be made under the same conditions with respect to the scan rate.

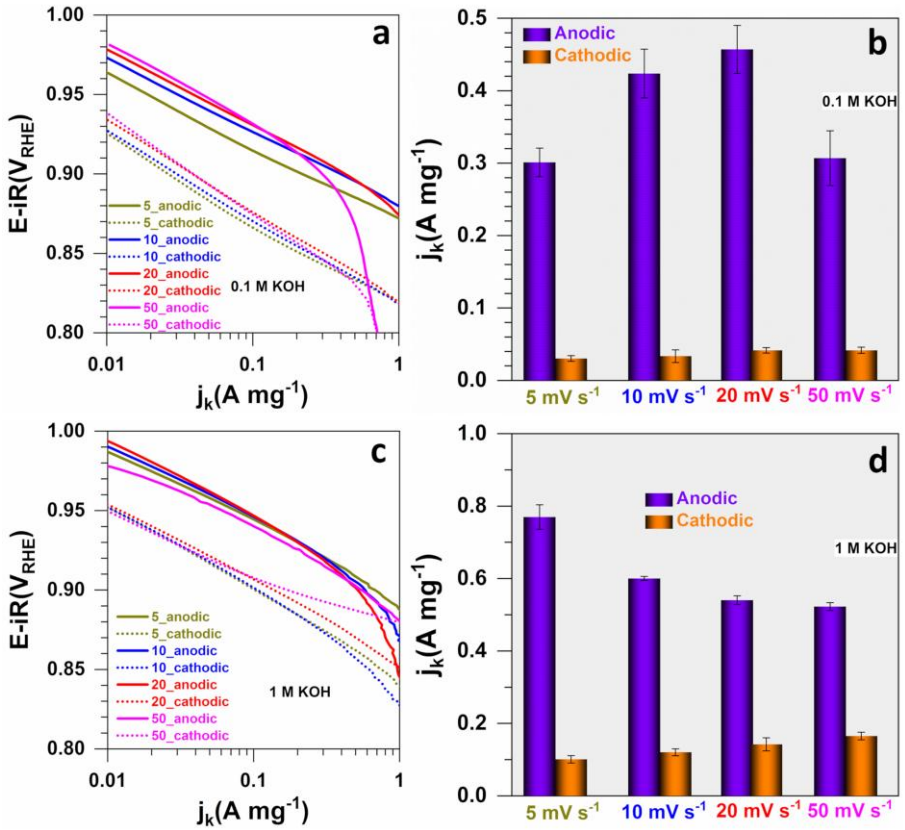

Figure 4. Effect of the scan rate from LSV (in mV s^{-1}) at 1600 rpm. (a) Tafel plots in 0.1 M KOH. (b) Kinetic current density at 0.9 V_{RHE} in 0.1 M KOH. (c) Tafel plots in 1 M KOH. (d) Kinetic current density at 0.9 V_{RHE} in 1 M KOH. Error bars represent 1 SD ($n \geq 3$).

Impact of the voltammetry method for: CV vs LSV. Having shown that the direction in which the potentials were scanned and the speed at which this scanning was done have a major impact on the magnitude of the kinetic parameters, we finally sought to know if the polarization method also has a substantial effect. It is worth of mentioning that practical fuel cells devices are tested using pseudo steady-state conditions (potentiostatic or galvanostatic) and even ORR was investigated by the potentiostatic polarization of stepwise potentials.[9]

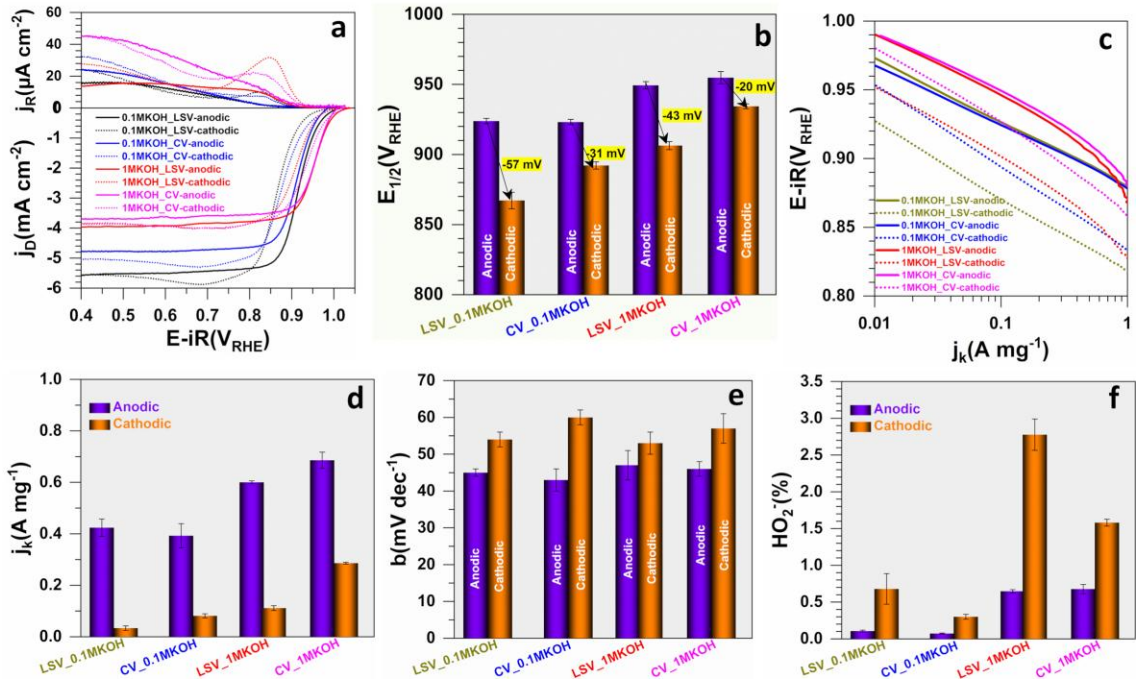

Figure 5. Effect of the voltammetry method. (a) LSV and CV polarization curves (1600 rpm, 10 mV s^{-1}) of ORR at an RRDE step up: disk (bottom) and ring (top). (b) Half-wave potential. (c) Tafel plots. (d) Kinetic current density at 0.9 V_{RHE}. (e) Tafel slope. (f) Incomplete hydroperoxide anion at 0.85 V_{RHE}. Error bars represent 1 SD ($n \geq 3$).

The outcomes are shown in Figures 5a-f and S12 (data are gathered in Table S1). There is still a big difference between the anodic and cathodic directions where the polarization curves are positively shifted towards high potentials when the electrode scanning starts at the lower potential limit and increases. For j_{diff}(mA cm^{-2}) = -5.6 (LSV) and -4.8 (CV) in 0.1 M KOH, the difference of 14% does not impact significantly the other quantitative metrics of the $E_{1/2}$ (Figure 5b), j_k (Figure 5c-d) and Tafel slope (Figure 5e). The big discrepancy is the amount of undesired HO_2^- (Figures 5f and S12) that increases with the augmentation of the electrolyte concentration. While this part again emphasizes the need to indicate the direction of the scan, the observed difference might result from the discrepancy between the two techniques where LSV allows to

get close to "steady-state" conditions.[6-7,9] Actually, half of a CV may not be merely associated with an LSV, which explains why LSV is very popular for the study of ORR, HER, OER, etc.

As a general discussion, the purpose of the present work is not to impose a method for choosing the scan direction but to reveal its impact and how to avoid the pitfalls of a conflicting comparison of ORR kinetic data at Pd-based electrocatalysts. There are two schools of thoughts, one in favor of the cathodic direction (decreasing potentials) and the other in favor of the anodic direction (increasing potentials). The defenders of the cathodic direction argue on the functioning of the fuel cell device where the voltage [$U = E_{(+)} - E_{(-)} = E_{(\text{cathode})} - E_{(\text{anode})}$] is maximum when each of the half-cells has its highest value, mathematically speaking, high for $E_{(\text{cathode})}$ and low for $E_{(\text{anode})}$. So, we should work by gradually increasing the overall cell voltage, thus decreasing $E_{(\text{cathode})}$, that of ORR. However, in practice, it may turn out that higher currents are required as we start operating a fuel cell, this is the argument of those in favor of the anodic direction. In the middle, one can rationally think that it would be better to do both directions during ORR. Then, we either report data for both directions, as is already done for the kinetic current density (j_k, A mg^{-1}_{metal} and A cm^{-2}_{ECSA}), or we represent only the average value, which is in fact already done during fuel cell tests. For metallic electrocatalysts (Pd herein and Pt elsewhere[9]), one thing is sure, the scan direction and the rate at which the potentials are run in that direction should be clearly indicated in the reports. The cathodic direction can start at an onset potential slightly positive from OCP, so, essential to disclose. We note that the activity discrepancy is expected for materials with surface reactions within the electrochemical window of ORR, that is, 0.5-1 V_{RHE}. We can see from the Figure 2b that the kinetics region of ORR is situated in the potential window where the surface of palladium is oxidized. Given that the surface reaction is affected by the reactivity of the electrocatalyt with the water molecules or electrolyte, the electrochemical

response corrolarely depends on the surface state. Therefore, OCP of O_2-saturated electrolyte is a mixed electrode potential between ORR and redox processes involving the surface species (M, $M(OH)_x$, MO_x). It means that the reduction thermodynamics and kinetics of ORR will, also, depend on those of the oxidized species $M(OH)_x$ and/or MO_x. So, OCP should not be used as a guarantee of performance. Finally, there is an appeal for other types of commonly used materials, for instance, the PGM-free electrocatalysts that present or not a surface oxidation-reduction profiles in the potentials range of interest for ORR, that is, 0.5-1 V_{RHE}.

To conclude, our results show that a possibly unintentional non-disclosure of all experimental conditions is very problematic when comparing ORR kinetic data of Pd-based electrocatalysts in alkaline electrolytes. Specifically, the used scan direction to record the polarization curves is generally ignored while the experimental data show that the anodic scanning (low to high potentials) leads to ultrafast electrocatalytic kinetics with a positive shift of the half-wave potential and the dramatic increase of the kinetic current density 4 to 15 times. The exact origin of this discrepancy is the surface state of the metallic electrocatalyst. The electrocatalysis research community needs to be careful to the likely over-/under-estimation of the ORR's figures of merit (kinetic current density, Tafel slope, half-wave potential and onset potential) before claiming any outstanding or superior performance whereas this could not be the case. The present work contributes towards the best practices and encourages every researcher to strike transparency and reproducible methodologies in electrochemical energy conversion systems.

ASSOCIATED CONTENT

Supporting Information. The following files are available free of charge

Experimental details, summary of ORR data from relevant Pd-based electrocatalysts at RDE/RRDE in alkaline media for the last years, (HR)TEM images, and extended Figures/Tables.

Notes

The authors declare no competing financial interest.

ACKNOWLEDGMENT

Y.H. thanks European Institute of Membranes of Montpellier (COGENFC, PAT-Energy-Axis-2018) and LabEx CheMISyst (ANR-10-LABX-05-01) for startup funds support. This work was financially supported by the Army Research Office MURI (W911NF-14-1-0263). This work was granted access to the France HPC resources of [CCRT/CINES/IDRIS] under the allocation 2020 [x2020087369] made by GENCI (Grand Equipement National de Calcul Intensif). The authors acknowledge Dr. Erwan Oliviero (MEA platform, Université de Montpellier) for TEM analysis.

REFERENCES

1. Jiao, K.; Xuan, J.; Du, Q.; Bao, Z.; Xie, B.; Wang, B.; Zhao, Y.; Fan, L.; Wang, H.; Hou, Z.; Huo, S.; Brandon, N. P.; Yin, Y.; Guiver, M. D., Designing the next generation of proton-exchange membrane fuel cells. *Nature* **2021,** *595* (7867), 361-369.
2. Debe, M. K., Electrocatalyst approaches and challenges for automotive fuel cells. *Nature* **2012,** *486* (7401), 43-51.
3. Yang, Y.; Chen, G.; Zeng, R.; Villarino, A. M.; DiSalvo, F. J.; van Dover, R. B.; Abruña, H. D., Combinatorial Studies of Palladium-Based Oxygen Reduction Electrocatalysts for Alkaline Fuel Cells. *J. Am. Chem. Soc.* **2020,** *142* (8), 3980-3988.
4. Lima, F. H. B.; Zhang, J.; Shao, M. H.; Sasaki, K.; Vukmirovic, M. B.; Ticianelli, E. A.; Adzic, R. R., Catalytic Activity−d-Band Center Correlation for the O2 Reduction Reaction on Platinum in Alkaline Solutions. *J. Phys. Chem. C* **2007,** *111* (1), 404-410.
5. Kocha, S. S.; Shinozaki, K.; Zack, J. W.; Myers, D. J.; Kariuki, N. N.; Nowicki, T.; Stamenkovic, V.; Kang, Y.; Li, D.; Papageorgopoulos, D., Best Practices and Testing Protocols for Benchmarking ORR Activities of Fuel Cell Electrocatalysts Using Rotating Disk Electrode. *Electrocatalysis* **2017,** *8* (4), 366-374.
6. Li, D.; Batchelor-McAuley, C.; Compton, R. G., Some thoughts about reporting the electrocatalytic performance of nanomaterials. *Applied Materials Today* **2020,** *18*, 100404.
7. Dix, S. T.; Lu, S.; Linic, S., Critical Practices in Rigorously Assessing the Inherent Activity of Nanoparticle Electrocatalysts. *ACS Catal.* **2020,** *10* (18), 10735-10741.
8. Mayrhofer, K. J. J.; Strmcnik, D.; Blizanac, B. B.; Stamenkovic, V.; Arenz, M.; Markovic, N. M., Measurement of oxygen reduction activities via the rotating disc electrode method: From Pt model surfaces to carbon-supported high surface area catalysts. *Electrochim. Acta* **2008,** *53* (7), 3181-3188.
9. Shinozaki, K.; Zack, J. W.; Richards, R. M.; Pivovar, B. S.; Kocha, S. S., Oxygen Reduction Reaction Measurements on Platinum Electrocatalysts Utilizing Rotating Disk

Electrode Technique: I. Impact of Impurities, Measurement Protocols and Applied Corrections. *J. Electrochem. Soc.* **2015,** *162* (10), F1144-F1158.
10. Siegmund, D.; Metz, S.; Peinecke, V.; Warner, T. E.; Cremers, C.; Grevé, A.; Smolinka, T.; Segets, D.; Apfel, U.-P., Crossing the Valley of Death: From Fundamental to Applied Research in Electrolysis. *JACS Au* **2021,** *1* (5), 527-535.
11. Cassani, A.; Tuleushova, N.; Wang, Q.; Guesmi, H.; Bonniol, V.; Cambedouzou, J.; Tingry, S.; Bechelany, M.; Cornu, D.; Holade, Y., Fe-Modified Pd as an Effective Multifunctional Electrocatalyst for Catalytic Oxygen Reduction and Glycerol Oxidation Reactions in Alkaline Media. *ACS Appl. Energy Mater.* **2021,** *4* (9), 9944-9960.
12. Luo, M.; Zhao, Z.; Zhang, Y.; Sun, Y.; Xing, Y.; Lv, F.; Yang, Y.; Zhang, X.; Hwang, S.; Qin, Y.; Ma, J.-Y.; Lin, F.; Su, D.; Lu, G.; Guo, S., PdMo bimetallene for oxygen reduction catalysis. *Nature* **2019,** *574* (7776), 81-85.
13. Yu, Z.; Xu, S.; Feng, Y.; Yang, C.; Yao, Q.; Shao, Q.; Li, Y.-f.; Huang, X., Phase-Controlled Synthesis of Pd–Se Nanocrystals for Phase-Dependent Oxygen Reduction Catalysis. *Nano Lett.* **2021,** *21* (9), 3805-3812.
14. Yu, H. J.; Zhou, T. Q.; Wang, Z. Q.; Xu, Y.; Li, X. N.; Wang, L.; Wang, H. J., Defect-Rich Porous Palladium Metallene for Enhanced Alkaline Oxygen Reduction Electrocatalysis. *Angew. Chem.-Int. Edit.* **2021,** *60* (21), 12027-12031.
15. Wang, L.; Zeng, Z.; Gao, W.; Maxson, T.; Raciti, D.; Giroux, M.; Pan, X.; Wang, C.; Greeley, J., Tunable intrinsic strain in two-dimensional transition metal electrocatalysts. *Science* **2019,** *363* (6429), 870-874.
16. Shao, M.; Peles, A.; Shoemaker, K., Electrocatalysis on Platinum Nanoparticles: Particle Size Effect on Oxygen Reduction Reaction Activity. *Nano Lett.* **2011,** *11* (9), 3714-3719.
17. Tateishi, N.; Yahikozawa, K.; Nishimura, K.; Takasu, Y., Hydrogen electrode reaction on electrodes of glassy carbon-supported ultrafine Pd particles in alkaline media. *Electrochim. Acta* **1992,** *37* (13), 2427-2432.
18. Hu, C.-C.; Wen, T.-C., Voltammetric investigation of palladium oxides—I: Their formation/reduction in NaOH. *Electrochim. Acta* **1995,** *40* (4), 495-503.
19. Grdeń, M.; Lukaszewski, M.; Jerkiewicz, G.; Czerwinski, A., Electrochemical behaviour of palladium electrode: Oxidation, electrodissolution and ionic adsorption. *Electrochim. Acta* **2008,** *53* (26), 7583-7598.
20. Gileadi, E., *Electrods Kinetics for Chemists, Chemical Engineers, and Materials Scientists*. Wiley-VCH: New York, N Y, USA, 1993; p 616.
21. Jeff Greeley; Jens K. Nørskov; Mavrikakis, M., Electronic structure and catalysis on metal surfaces. *Annual Review of Physical Chemistry* **2002,** *53* (1), 319-348.
22. Yang, Y.; Peng, H.; Xiong, Y.; Li, Q.; Lu, J.; Xiao, L.; DiSalvo, F. J.; Zhuang, L.; Abruña, H. D., High-Loading Composition-Tolerant Co–Mn Spinel Oxides with Performance beyond 1 W/cm2 in Alkaline Polymer Electrolyte Fuel Cells. *ACS Energy Lett.* **2019,** *4* (6), 1251-1257.
23. Davis, R. E.; Horvath, G. L.; Tobias, C. W., The solubility and diffusion coefficient of oxygen in potassium hydroxide solutions. *Electrochim. Acta* **1967,** *12* (3), 287-297.